Meteorology and Atmospheric Physics (2019) 131:613–626
https://doi.org/10.1007/s00703-018-0594-5

ORIGINAL PAPER

Characteristics of tropical cyclone extreme precipitation and its preliminary causes in Southeast China

Wenyu Qiu[1,2] · Fumin Ren[2] · Liguang Wu[1,2] · Lianshou Chen[2] · Chenchen Ding[2,3]

Received: 27 June 2017 / Accepted: 17 February 2018 / Published online: 1 March 2018

Abstract
Extreme precipitation induced by a tropical cyclone (TC) is of great concern to Southeast China. Regional characteristics of daily TC-induced extreme precipitation (TCEP) between 1958 and 2016 and the associated preliminary causes over Southeast China (Zhejiang, Fujian, and Shanghai) were examined by applying the objective synoptic analysis technique, TC track similarity area index, daily precipitation observations, and reanalysis data. The intensity and frequency of high-intensity TCEP (≥ 100, ≥ 200, ≥ 300 mm) have had an increasing trend over recent decades. Most of TCEP occurs from July to September, with frequency peaks in August for TCEP at all intensity levels, apart from the frequency for TCEP ≥ 300 mm that peaks in September. Regions with high frequency and large TCEP (R-HFLTs) (relatively high frequency for TCEP ≥ 100 mm) were concentrated along the coastline of the southern coastal Fujian (Southern R-HFLT), the regions from northern coastal Fujian to southernmost coastal Zhejiang (Central R-HFLT), and central coastal Zhejiang (Northern R-HFLT), decreasing from the coastline to inland. The Central R-HFLT region had the highest TCEP intensity and frequency for TCEP ≥ 100 mm compared with the other R-HFLTs. Further analysis showed that the special terrain of Southeast China matched the spatial distribution of TCEP, which highlights the significance of the topography of Southeast China. To discover other factors responsible for the heavy TCEP, we compared two TC groups that influence Central R-HFLT. Under a more northerly direction and slow movement combined with the unique terrain, TCs with stronger vortex circulation generated heavier TCEP during landfall in Central R-HFLT. Heavy TCEP occurred with easterly and southeasterly winds interacting with terrain over the eastern coast for Central R-HFLT. Although large changes in the internal and external environment were sensitive to the observed TCEP intensity, the interaction between TC circulation and the complex topography in Southeast China under the northerly track was the dominant factor.

1 Introduction

Among the most devastating natural disasters (Shah 1983; Zhang et al. 2009), tropical cyclones (TCs), are mainly associated with torrential rainfall in China, which causes widespread flooding and landslides (Chen and Ding 1979; Chen 2007). Extreme weather events caused by TC-induced extreme precipitation have received much attention, including typhoons Haiyan (2013), Morakot (2009), and Fitow (2013). They all resulted in great loss of human life and severe property damage due to heavy rainfall. With the ongoing development of coastal areas, knowledge of the specific characteristics of the TC-related torrential rainfall along coastal regions that experience the heaviest precipitation is, therefore, important in disaster mitigation.

TC precipitation (TCP) and climate variation have been investigated in the North Pacific (Rodgers et al. 2000) and North Atlantic (Rodgers et al. 2001) basins; the western North Pacific (Kubota and Wang 2009); China, including Taiwan and the Hainan Islands (Ren et al. 2006); Southern China (Chan et al. 2004); and in specific studies on Hong Kong (Li et al. 2015), Hainan Island (Wu et al. 2007) and Taiwan Island (Chang et al. 2013; Wu et al. 2016). Southeast

Responsible Editor: M. Kaplan.

✉ Fumin Ren
fmren@163.com

[1] Key Laboratory of Meteorological Disaster, Ministry of Education (KLME), Pacific Typhoon Research Center (PTRC), Nanjing University of Information Science and Technology, Nanjing, China

[2] State Key Laboratory of Severe Weather, Chinese Academy of Meteorological Sciences, Beijing 10081, China

[3] School of Atmospheric Science, Chengdu University of Information Technology, Chengdu, China

China, which includes Zhejiang and Fujian provinces and Shanghai City (Fig. 1), is characterized by complex terrain and includes a coastline that is most frequently and severely affected by TCs on a global scale. Previous studies have produced conflicting results of the TCP trend over Southeast China. Observed TCP in China suggests decreasing trends in the proportion of total precipitation and frequency of torrential rain (Cheng et al. 2007; Ren et al. 2006), while the long-term trend of TCP (Liu et al. 2013) and the trend of the spatial pattern for rainfall intensity (Ying et al. 2011) are increasing in Southeast China. Zhang et al. (2013) found that the average rainfall per TC has significantly increased in Southeast China during 1965–2009.

The spatial distribution of TCP varies greatly between locations (Knight and Davis 2009), on a monthly basis (Larson et al. 2005; Knight and Davis 2007; Jiang and Zipser 2010), and between individual storms. The amount and frequency distribution of coastline TCP are characterized by high asymmetry relative to the TC track due to the combined effect of land interaction, storm motion, and vertical wind shear (Chan et al. 2004; Liu et al. 2007). Lin et al. (2001) and Ge et al. (2010) emphasized the important role of the topography in producing heavy rainfall. Zhu et al. (2010) used satellite data to show that the interaction between TC circulation and the complex coastal terrain along the coast of Eastern China can significantly enhance precipitation. In case studies, such as, Bilis (2006) (Gao and Meng 2009); Morakot (2009) (Wu et al. 2011; Lee et al. 2011; Xie and Zhang 2012; Yu and Cheng 2013); and Haitang (2005) (Yue et al. 2008), factors, including multiscale monsoonal influence, abundant moisture supply from the southwesterly winds, vertical wind shear, storm motion, and topographic effect, were important for the asymmetric distribution of TCP.

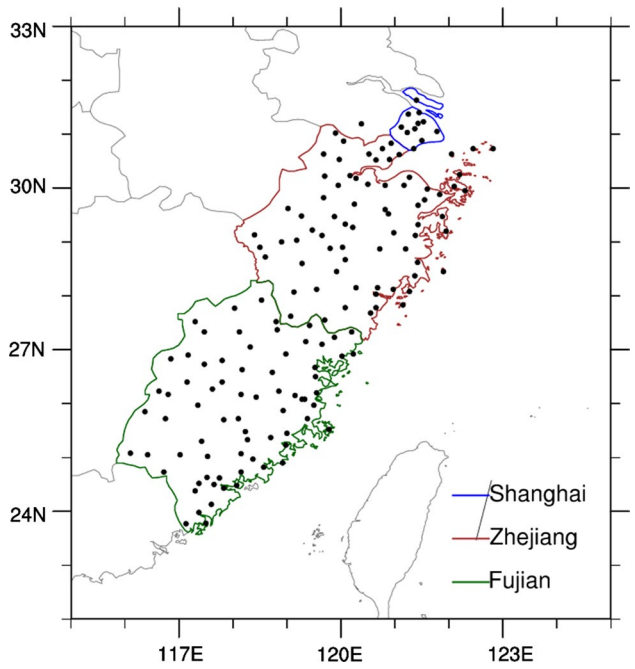

Fig. 1 Distribution of the 157 meteorological stations in Southeast China, including Zhejiang and Fujian provinces, and Shanghai City

Chang et al. (2012) found that TCP contributes more to extreme precipitation than to total precipitation, and the heavy rainfall often results in severe loss of life and property. Therefore, focus should be on the TC-induced extreme precipitation (TCEP). While total TCP has been studied in detail, including information on, for example, the 95th percentile, average precipitation per typhoon, annual mean precipitation, and monthly precipitation, previous work has not addressed the potential changes in extreme precipitation produced by TCs. It has been predicted that the destructiveness of TCs will increase because TC intensity shows an increasing trend under global warming (Webster et al. 2005; Knutson et al. 2010; Wu and Zhao 2012). However, it is not clear whether TCEP induced by TCs is increasing. To date, the change in TCEP in Southeast China is not well understood. The TCEP in this study emphasizes two points: Firstly, it belongs to extreme precipitation; Secondly, it is caused by TCs. From the threshold of 95% (Fig. 1a in Su et al. 2016) and the ratio of 50 mm to all precipitation (not shown), the absolute threshold of 50 mm could reflect the extreme precipitation of stations. Exploring TCP above 50 mm could gain a general understanding of extreme precipitation induced by TCs. Defining TCEP as TC-induced daily precipitation above 50 mm, we conducted a regional study on TCEP in Southeast China. To understand the effect of TCEP in this region, the general characteristics of TCEP, including temporal trends and spatial distribution, and preliminary causes, were examined on the basis of daily station precipitation together with TC track data for the Northwest Pacific basins during 1958–2016. First, an accurate understanding of the climate variation of the TCEP in Southeast China was established. Then, different from the usual case studies, we analyzed the spatial distribution of TCEP using climate data, from the perspective of the high frequency distribution at high precipitation intensities. Some cause analysis was carried out on the spatial distribution of TCEP. The rest of the paper is organized as follows. Data and methods are described in Sect. 2. Section 3 provides the specific demonstration of the spatial and temporal characteristics of TCEP. Based on the spatial distribution in Sect. 3, Sect. 4 reveals some possible causes. The results and discussion are presented in Sect. 5.

2 Data and methods

2.1 Data

The main precipitation observation is daily precipitation from a total of 157 meteorological stations in Southeast China provided by the National Meteorological Information

Center from the China Meteorological Administration (CMA), with the measurement coverage ranging from 12 UTC on the previous day to 12 UTC on the present day. As illustrated in Fig. 1, the stations in Southeast China cover the coastal areas of Zhejiang and Fujian provinces and Shanghai City. TC best track data were obtained from the Shanghai Typhoon Institute of CMA, including observed TC location and intensity (maximum 2-min surface wind speeds and minimum central pressure) in the Western North Pacific basin (Western North Pacific and South China Sea) at 6-h intervals.

The data associated with causal analysis were derived from three datasets: the global reanalysis data from the National Centers for Environmental Prediction–National Center for Atmospheric Research (NCEP–NCAR) reanalysis, with 2.5° × 2.5° grid spacing and 26 vertical layers at 6-h intervals; and the high-resolution European Centre for Medium-Range Weather Forecasting (ECMWF) datasets, known as ERA-40 data and ERA-Interim data. ERA-40 data are available between September 1957 and August 2002, and ERA-Interim data are available from January 1979 to December 2016. Since neither ERA-40 data nor ERA-Interim data can completely cover 1958–2016, we use a collection of data between 1958 and 1978 in ERA-40 and data between 1979 and 2016 in ERA-interim. Both datasets have a resolution of 1° × 1°, including horizontal wind field, vertical velocity field, geopotential height field, temperature field, and the specific humidity field from sea level pressure at 850, 500, and 200 hPa.

2.2 Methods

Daily torrential rainfall was defined as the 24 h accumulated precipitation that reaches at least 50 mm or more in the weather forecast. The extreme effect of TCEP on Southeast China was demonstrated in terms of the TC case maximum daily torrential rainfall (TCMDTR) and the station daily torrential rainfall associated with TCs (SDTR). TCEP refers to total TC-related daily torrential rainfall, TCMDTR is the maximum produced by each TC, and SDTR records daily torrential rainfall at each station. TCMDTR and SDTR both measure TCEP except from different aspects. In this study, the influential TCs were defined as those producing precipitation for at least one station in Southeast China. Extreme TCs were defined as influential TCs associated with TCEP. One extreme TC may result in several SDTR data points, but only one TCMDTR data point. We analyzed the climatic characteristics of TCEP from the perspective of the TCMDTR and studied the spatial distribution characteristics of TCEP using TCMDTR and SDTR.

The aim of this study was to identify the TCEP over Southeast China and analyze the characteristics and causes of the spatial distribution of TCEP. As an initial step, an objective procedure called the objective synoptic analysis technique (OSAT) (Ren et al. 2001) was used to identify the total TC-induced rainfall and associated influential TCs in Southeast China between 1958 and 2016. Then, based on the influential TCs list and the spatial distribution of TCEP, the tropical cyclone track similarity area index (TSAI) method (Ren et al. 2017) was applied to form two TC groups, which had a similar track but caused TCEP at different intensity levels, which will be described in detail in Part 4. The two groups were used to analyze the causes of the TCEP in Central R-HFLT. Based on the cause diagnosis, because TCs are moving systems, a dynamic composite analysis (Gray 1981; Li et al. 2004) that synthesizes atmospheric variables by tracing progressive TC centers was performed to extract common circulation features during the duration of the TC. The average result of the five members in each group after dynamic composite analysis was considered to represent one category.

3 Characteristics of TCEP

The TCs that influence China always have three prevailing tracks according to Wu et al. (2005). For Southeast China, the influential TCs move northwestward and often follow a more easterly track passing over, or near, Taiwan. They frequently make landfall on the southeastern coast of China and bring extreme precipitation. During 1958–2016, the total number of TCs that developed in the Northwest Pacific and South China Sea was 1908. Only 743 were identified as influential TCs, making up 36.7% of the total. There were 478 extreme TCs that produced TCEP, covering 64.3% of the total influential TCs. The characteristics of TCEP can be derived from the temporal variation and spatial distributions.

3.1 Temporal characteristics

Observational studies often focus on the precipitation intensity and its frequency. Using the identification results, we produced TC rankings based on TCMDTR data (Table 1 lists the first 15 TCs). The 15 typhoons, where TCMDTR was above 300 mm, represent the influential TCs with the strongest effect over Southeast China. The list includes well-known typhoons, such as Haitang (2005), Morakot (2009), and Bilis (2006). Haitang (2005) produced TCEP with the highest intensity reaching 472.5 mm, and Typhoon Morakot (2009) resulted in a large TCEP of 415.2 mm on mainland China after causing the well-known world-breaking extreme precipitation in Taiwan. The total number of typhoons from July to September was 13, with the highest number of typhoons occurring in September. Southeast China is more prone to high TCEP in September. A close inspection of the data reveals that seven of the 15 typhoons occurred

Table 1 Ranking list of the first 15 TCs based on the TC maximum daily torrential rainfall (TCMDTR) over Southeast China

Ranking	TC name	Life time	TMDP (mm)	Corresponding station
1	Haitang	2005.07.12.08-07.20.14	472.5	Zherong
2	Morakot	2009.08.03.14-08.13.14	415.2	Zherong
3	Wendy	1999.09.01.14-09.06.14	403.8	Wenzhou
4	Fitow	2013.09.30.20-10.07.08	395.6	Yuyao
5	Amy	1977.08.16.14-08.27.20	394.5	Baoshan
6	Morakot	2003.08.01.02-8.05.08	392.4	Nanan
7	Lisa	1996.08.05.02-08.08.08	384.1	Changting
8	Elsie	1969.09.16.08-10.02.08	381.7	Zherong
9	Megi	2016.09.23.08-09.29.02	379.6	Wencheng
10	Linfa	2009.06.17.14-06.25.08	350.4	Dongshan
11	York	1999.09.12.14-09.17.14	347.2	Changle
12	Bilis	2006.07.08.14-07.17.20	346.2	Changtai
13	Herb	1996.07.23.08-08.04.02	344.9	Zherong
14	Wilda	1973.06.28.14-07.06.08	330.2	Pingyang
15	Bess	1971.09.17.08-09.27.02	322.1	Zherong

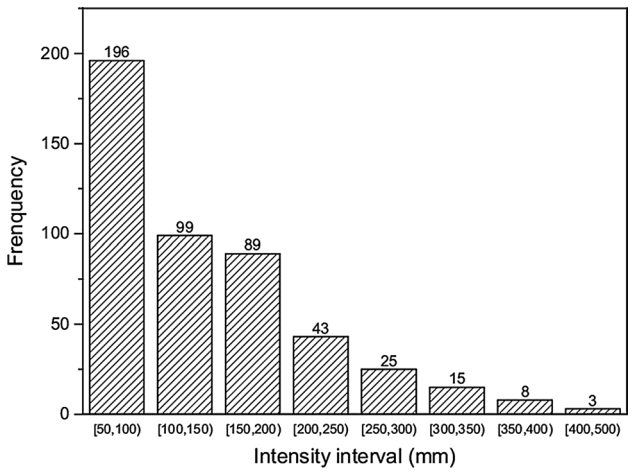

Fig. 2 Frequency distribution of TCMDTR (mm) at different intensity intervals during 1958–2016 over Southeast China

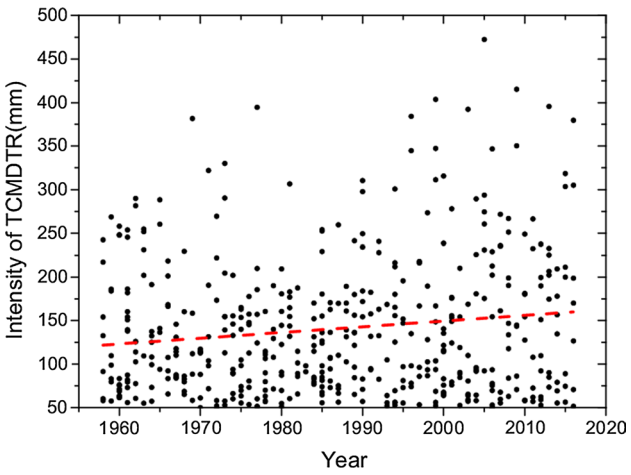

Fig. 3 Time-intensity distribution of TCMDTR ≥ 50 mm during 1958–2016 over Southeast China. The red dashed line indicates the average trend of intensity with time

after 2000, partially reflecting the fact that the intensity of extreme precipitation brought by TCs has been increasing in recent years.

The frequency of the TCMDTR at different levels was fairly dissimilar. In general, the frequency decreased as the intensity increased, displaying a ladder-type pattern (Fig. 2). Among the 478 extreme TCs that caused TCMDTR over 50 mm, there were 196 TCEP measuring between 50 and 100 mm, accounting for 41% of the total; 282 for TCEP ≥ 100 mm, 94 for ≥ 200 mm, 26 for ≥ 300 mm, and 3 for ≥ 400 mm, accounting for 59, 19.7, 5.4, and 0.63%, respectively. The damage resulting from a TCP was mainly caused by the few TCs with relatively large TCMDTR. Considering the frequency distribution of TCMDTR for different intensity intervals, TCEP was divided into the following groups for discussion: TCEP ≥ 50 mm, TCEP ≥ 100 mm, TCEP ≥ 200 mm, and TCEP ≥ 300 mm.

TCEP intensity generally showed a significant increase, which was studied in more detail. Figure 3 presents the annual distribution of TCMDTR at different intensity levels caused by each influential TC. An increasing trend, which is statistically significant at a level of 0.01, is shown by the red dashed line, with the TCMDTR scattered at higher intensity levels over the past few years. For example, most of TCMDTR above 300 mm occurred after 1995.

As the overall contribution of TCEP depends on the combined effect of frequency and rainfall intensity, then we focused on the frequency. The time series of the four groups of TCMDTR along with their respective linear trends are plotted in Fig. 4. The total number of extreme TCs has

decreased slightly (not statistically significant) over recent years (Fig. 4a), which is consistent with the finding that the average frequency of TCs will decrease under global warming (Knutson et al. 2010) and the results of Ren et al. (2006). However, the number of extreme TCs with TCMDTR above 100 mm suggests a significant increasing trend over the past 59 years, which agrees with the trend of average rainfall per TC according to Zhang et al. (2013). Specifically, the occurrence of TCMDTR ≥ 100 mm shows a weaker increasing trend of 0.06/decade (Fig. 4b), which is not statistically significant. By contrast, the frequency of TCMDTR ≥ 200 mm (≥ 300 mm) shows an increasing trend of 0.22/decade (0.18/decade) over the past 59 years (Fig. 4c, d), which is statistically significant at a level of 0.05 (0.01). The greater the intensity level, such as 200 or 300 mm and above, the more obvious the upward trend. In particular, after 2000 a significant increase occurred for TCMDTR ≥ 200 mm (Fig. 4c) and TCMDTR ≥ 300 mm (Fig. 4d).

On an annual timescale, the intensity and frequency of TCEP in Southeast China increased with time, which confirms that extreme TCs have a growing impact on Southeast China.

The monthly variation of TCEP in Southeast China shared similar characteristics with the TC activity. TCMDTR ≥ 50 mm occurred mainly between April and November, while TCMDTR over 100 mm occurred mainly between May and October (Fig. 5). The monthly changes of frequency exhibited a single peak for TCMDTR with different intensity levels during 1958–2016 (Fig. 5), with the peak season from July to September. In particular, TCMDTR occurrence at all intensity levels peaked in August, except for the peak for TCMDTR ≥ 300 mm occurring in September, which is consistent with the results in Table 1. The number of TCMDTR between 50 and 100 mm was comparable with the number of TCMDTR between 100 and 200 mm during June to October. April was the first month when

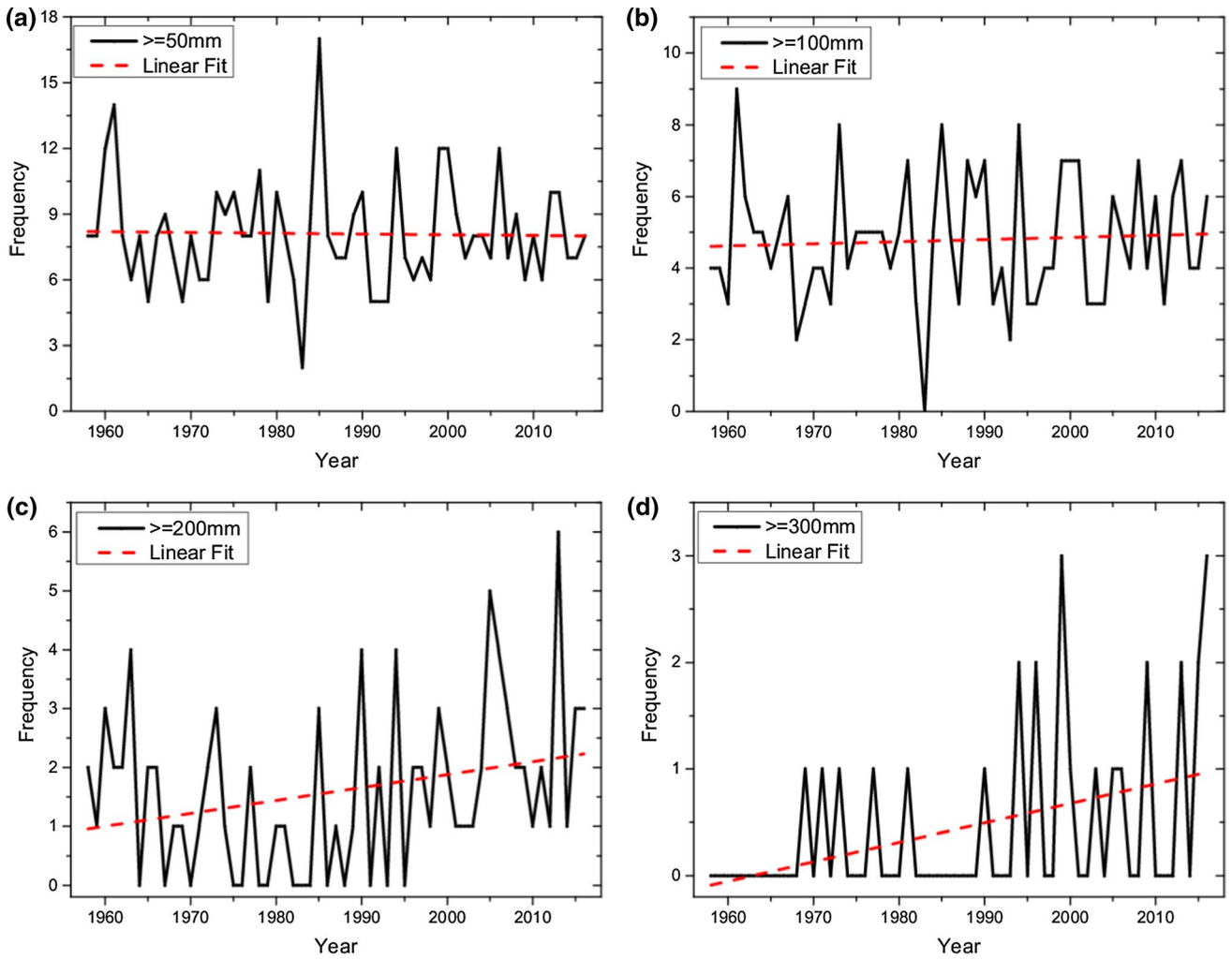

Fig. 4 Annual variations of TCMDTR (mm) frequency and the linear trends at different intensity levels over Southeast China during 1958–2016. **a–d** Are the frequencies for TCMDTR ≥ 50, ≥ 100, ≥ 200, and ≥ 300 mm, respectively

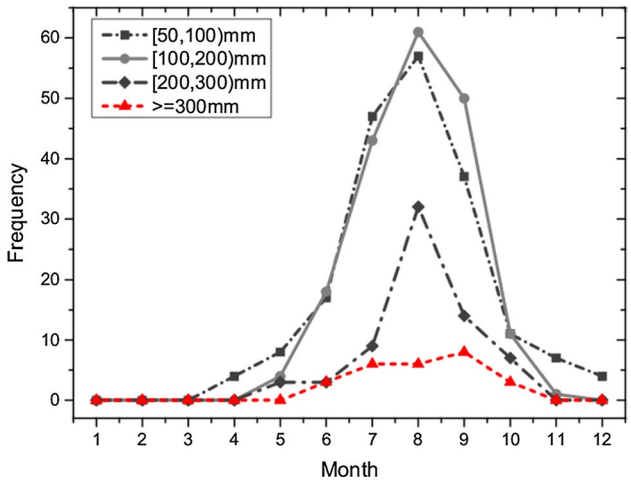

Fig. 5 Monthly variations of TCMDTR frequency at different intensity intervals during 1958–2016 over Southeast China

extreme TCs began to affect Southeast China, and TCEP over 100 mm occurred from May onwards. TCEP ≥ 100 mm no longer affected Southeast China after November, while extreme TCs still occurred until December. After reaching a peak in August, the frequency decreased rapidly, with the accumulated frequency of TCMDTR ≥ 50 mm from July to September accounting for 83% of the total. Therefore, the extreme TC season for Southeast China can be approximately divided into an early season (May–June), peak season (July–September), and late season (October–November). In general, TC activities dominate the monthly variation of TCEP occurrence in Southeast China.

3.2 Spatial characteristics

Spatial characteristics are intuitive and reflect the general features of TCEP along the southeast coast. For the spatial distribution of TCEP, we focused on regions where large TCEP always occurred, which we called regions with high frequency and large TCEP (R-HFLTs).

The frequency distribution of high TCEP was dissimilar for TCEP with different intensity levels, and the frequency of TCEP ≥ 100 mm was selected as representative of frequency of high-level TCEP. Figure 6, therefore, presents the spatial distribution of the occurrence frequency of SDTR ≥ 100 mm (Fig. 6a) and TCMDTR ≥ 100 mm (Fig. 6b) for all stations during 1958–2016, displaying an uneven pattern of a decrease from coastal to inland regions. As in Fig. 6a, high SDTR frequencies, for example, frequency larger than 40, were more concentrated in the three R-HFLTs: the southern coastal Fujian (Southern R-HFLT), the area from northern coastal Fujian to southernmost coastal Zhejiang (Central R-HFLT), and central coastal Zhejiang (Northern R-HFLT). Specially, the southern dividing line and the northern dividing line correspond to the location of Minjiang and Oujiang River, respectively. With the increase in intensity, the high frequencies tended to concentrate in the Central R-HFLT, showing that this area experienced TCEP with the highest frequency and the largest intensity. Similar spatial characteristics were discovered for TCMDTR in Fig. 6b, as frequencies larger than 4 for TCMDTR ≥ 100 mm are located in similar regions. Thus, stations in the three R-HFLTs discussed in this paper meet the condition for either frequency ≥ 40 for SDTR ≥ 100 mm

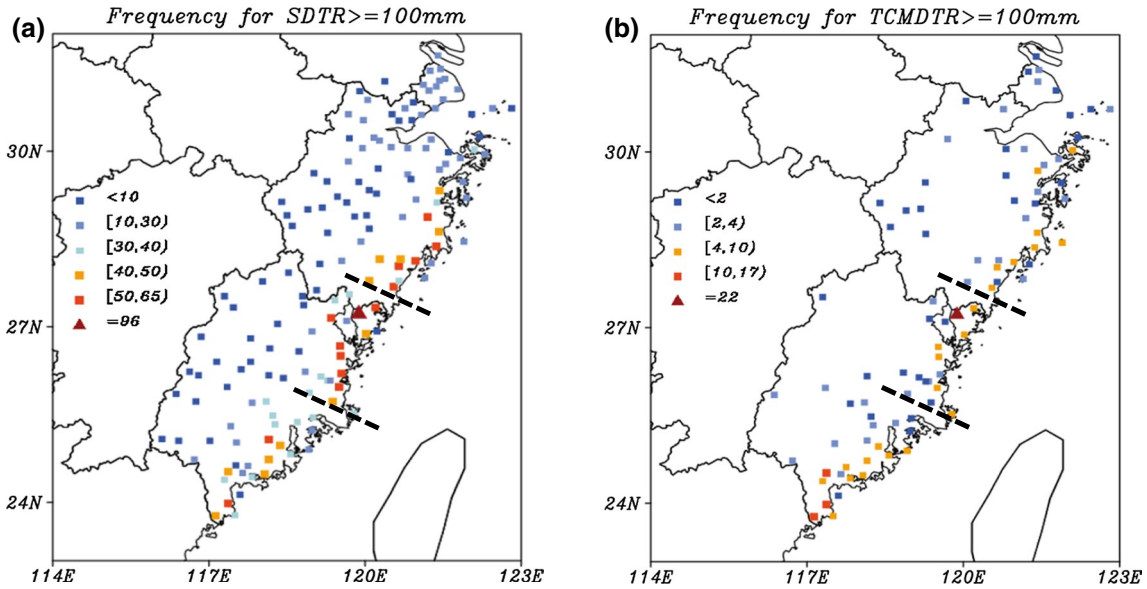

Fig. 6 Spatial frequency distributions for SDTR ≥ 100 mm (**a**) and TCMDTR ≥ 100 mm (**b**) over Southeast China during 1958–2016. The black dotted lines are the northern and southern dividing line of the three R-HFLTs

or frequency ≥ 4 for TCMDTR ≥ 100 mm. On the basis of both SDTR and TCMDTR, Zherong station (indicated by the triangle in Fig. 6) in Central R-HFLT experienced the most frequent TCEP.

4 Preliminary causes of TCEP

Based on the spatial distribution of TCEP in Sect. 3, we carried out some causal diagnoses to investigate possible causes for TCEP over Southeast China.

Terrain is considered an important factor for TCEP induced by influential TCs. As a TC makes landfall, it is often affected by land surface conditions, including coastal and inland topography and associated mesoscale processes (Meng and Wang 2016). Several studies on heavy TC rainfall in Taiwan (Wu et al. 2002; Lin et al. 2002; Cheung et al. 2008) have indicated that the special terrain of Taiwan Island, including a central mountain with an altitude of over 4 km, significantly affects the rainfall distribution through interactions with the typhoon circulation. Similarly, it is necessary to examine the effect of hilly terrain on TCEP on the southeast coast of China. The three R-HFLTs derived from Sect. 3 were consistent with topography (Fig. 7a) based on the geographical distribution of TCEP. While Southern R-HFLT is located on the central-to-southern coast of Daiyun Mountains in Fujian, Central R-HFLT coincides with the coastal area from South Yandang Hill in Southern Zhejiang to the northeast of Jiufeng Mountains in Northeast Fujian. Northern R-HFLT corresponds to the North Yandang Hill in the central areas of Zhejiang. The red symbols in Fig. 7a, which indicate either frequencies larger than 40 for SDTR ≥ 100 mm (Fig. 6a) or frequencies larger than 4 for TCMDTR ≥ 100 mm (Fig. 6b), were confined to the coastal slopes on the eastern side of the mountain. By averaging the horizontal winds at 925 hPa caused by the extreme TCs at each station in the TCEP days, we can get a composite horizontal wind distribution in the three R-HFLTs (Fig. 7b). Taking Zherong station (indicated by the relatively bigger circle in Fig. 7b) for example, there are totally 22 TCs that having caused TC case maximum daily torrential rainfall (TCMDTR) (Fig. 6b). Using the wind in the nearest grid of Zherong station to represent the station wind, the composite horizontal wind for Zherong station is calculated by the average wind at 925hPa in the TCEP day for all 22 TCs. As can be seen in Fig. 7b, 35 out of 36 station winds in the three regions have the eastward component. Specifically, the easterly winds correspond to Central R-HFLT, the southeast winds correspond to Southern R-HFLT, and the southeast winds or the northeast winds to Northern R-HFLT. Inferring from the configuration of the terrain (Fig. 7a) and the wind direction (Fig. 7b), most of the stations are on the windward

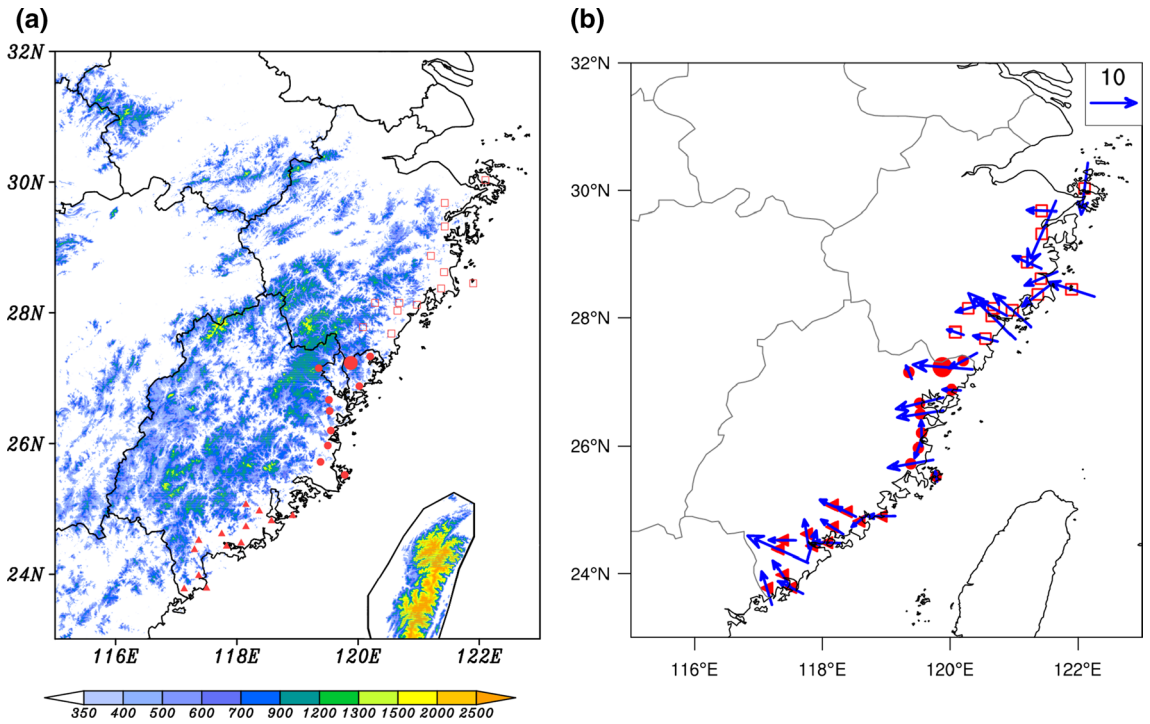

Fig. 7 Topographic map (**a**) and composite station wind field (vectors, units: m/s) at 925 hPa (**b**) of Southeast China with red symbols indicating the three R-HFLTs of TCEP. The solid circle represents the Central R-HFLT with relatively bigger circle represents Zherong station, the solid triangle represents the Southern R-HFLT, and the hollow rectangle represents the Northern R-HFLT

slope on the day when TCEP occurs, emphasizing the significance of topographic enhancement in causing extreme precipitation. For Southeast China, the terrain on the windward coastline slopes produce forced uplift and convergence, which contributes to the higher intensity and frequency of heavier rainfall in the coastal area compared with inland.

The three R-HFLTs have a good correspondence with the terrain, especially for the Central type. Located at the junction of the two provinces, where there is a valley between the mountains, Central R-HFLT has stations in the valley as well as the windward slope near the valley (Fig. 7a). The most typical station in the Central R-HFLT, Zherong station, is especially terrain specific. The highest point in Zherong county is 1479 m on the east side with an average height of 600 m and the elevation of Zherong station is 684 m. Surrounded by mountains with the southeastern side of the mountain higher than the northwest, Zherong station stands in a mountaintop basin, like a concave-shape or a "pocket" standing in a high altitude. In particular, in the corners between mountains around Zherong station, there are slits or gaps that help the wind enter the mountaintop basin, resulting small-scale vortex. This unique terrain including elevation, basin and slips is not only conducive to terrain uplift, but also contributes to small and medium scale processes, like local heavy rain with instability. From the station wind distribution, we see Zherong station corresponds to the strong easterly wind (Fig. 7b), of which the eastward component is 13.15 m/s, the highest among all the stations. The eastward wind could enter the basin from the slits and play a role with terrain. The combination of the eastward wind and the special topography produced stronger TCEP and higher frequency heavy rain. The frequency peak for SDTR $\geq$ 100 mm was 96 and the frequency peak for TCMDTR $\geq$ 100 mm was 22 at Zherong station (Fig. 6a, b), which were both far greater than the values at other stations. Great TCEP occurs when such a terrain hit a strong easterly wind. As a result, precipitation during July to September was characterized by large and sudden precipitation with transient changes, accounting for 41.3% of annual rainfall and July to September is called the typhoon thunderstorm season for Zherong. The concave terrain is very conducive to precipitation enhancement, which can also be shown by the "67.10" rainstorm event caused by storm "6718 Carla" in Xinliao in Taiwan. The TCEP, producing 1672 mm during 24 h (Chen et al. 2004), occurred on "pocket" terrain. We conclude that the terrain in Southeast China plays a key role in the formation of TCEP, especially for Central R-HFLT.

There is a strong positive correlation between the intensity and the frequency of TCEP $\geq$ 50 mm for the 157 stations over Southeast China (Fig. 8). With the increase of TCEP intensity, the frequency of TCEP at this station also tended to increase. Furthermore, among all 157 points, the top right point in Fig. 8 represents the extreme value of Zherong station, which is very prominent. The climatological features of TCEP distributions over Southeast China were highly modulated by the topography of the Southeast China coast.

Observations have demonstrated that strong TC circulation dynamically organizes deep convection and thus produces associated intense rainfall near the TC core (Burpee and Black 1989; Marks 1985), which leads to a strong dependence of rainfall on the TC track. For convenience, we classified extreme TCs affecting the three R-HFLTs into three groups: the north-type TCs, the central-type TCs, and the south-type TCs. An inspection of the features of the top ten TCs in each group suggests that the central-type TCs have the most prominent features. First, the central-type TCs displayed the strongest intensity among the three groups. Second, the central-type TCs had consistent tracks in common, while the tracks of the TCs in the other regions were complex. Figure 9 shows the tracks during the day when the TCEP occurred (hereafter the TCEP day) for the three groups ranked in the top ten. The influence of the TC track on the three R-HFLTs was different. The central-type TCs were mostly moving north–northwestward when making landfall in Fujian Province after landfall in Taiwan, except for one case (Fig. 9b). Most of the north-type TCs travelled northwestward making landfall on the southeast coast, but with scatted locations and few landfalls in Taiwan, while the tracks of the south-type TC were mostly northbound originating from the South China Sea. The central-type TCs produced extreme precipitation on the landfall day.

The central-type TCEP was the strongest, the terrain of the Central R-HFLT was special, and the tracks of the central-type TCs were consistent. Considering these aspects, the central type was therefore selected to investigate the effects of the TC characteristics and environmental factors on

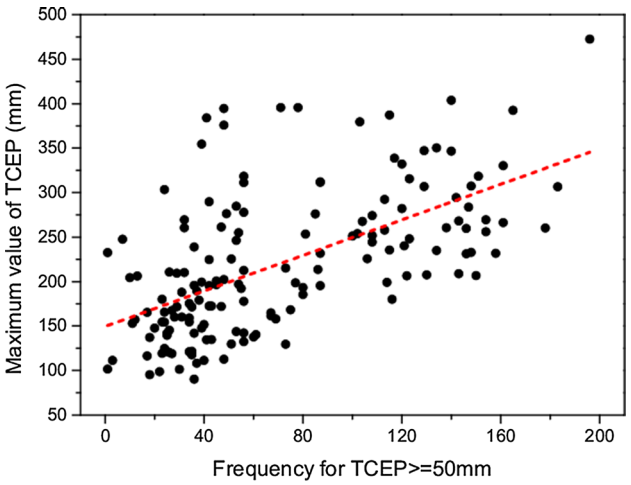

Fig. 8 Frequency–intensity distribution of TCEP $\geq$ 50 mm in Southeast China. The red dashed line indicates the linear fit

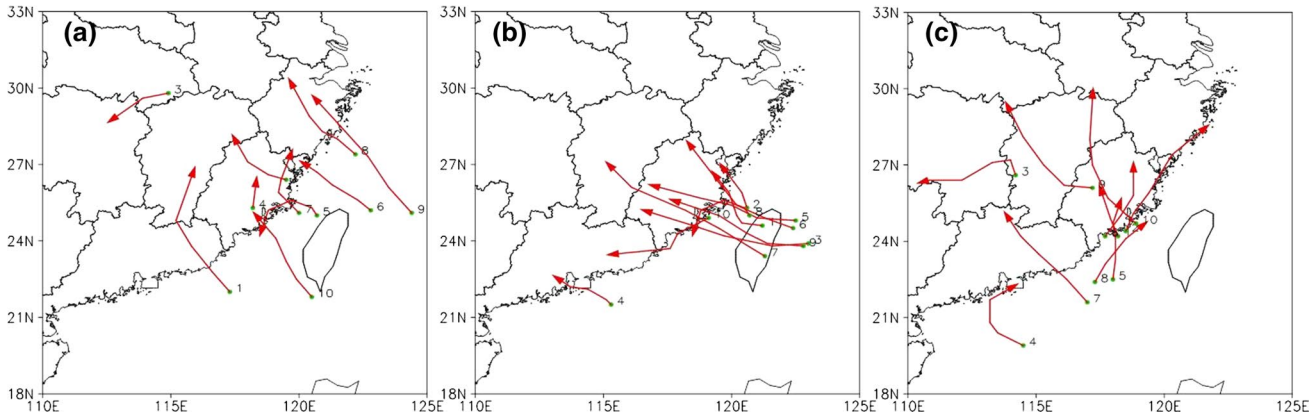

Fig. 9 Tracks of the top ten TCs of the north- (**a**), central- (**b**), and south-types (**c**) during the TCEP day

TCEP. As presented in Sect. 2, two TC groups of the central-type TCs [strong central-type TCs group (STG) and weak central-type TCs group (WTG)] were categorized (Table 2).

Here, we introduce the specific selection methods of these two TC groups. First of all, for the TCs affecting Central R-HFLT, the Typhoon Haitang (2005) brings the highest TCMDTR in the northwestward landfalling track, which is a typical heavy rainfall TC that affects Central R-HFLT in strong central-type TCs group. Choosing Haitang as the reference TC, the TSAI between the reference TC and the other all 743 influential TCs is then calculated and ranked. Second, among the 15 TCs (including Haitang) having the most similar tracks as Haitang, two appropriate groups of TCs with different TCMDTR values were selected. Five TCs with strong rainfall are selected as STG, and five TCs with weaker rainfall as the WTG. As a result, two TC groups, whose information is in Table 2, have similar tracks but cause TCEP at fairly different intensity levels. For STG, the daily rainfall maximum is 472.5 mm and the minimum is 266.9 mm; whereas for WTG, the maximum rainfall is 189.9 mm and the minimum is 155.8 mm. However, both two groups have produced TCEP.

To examine the wind-terrain effect on TCEP intensity, Fig. 10 displays the composite horizontal wind field at 850 hPa and the corresponding tracks of the two central-type TC groups with TCMDTR distribution on the TCEP day. As there are 5 time points of each TC track on the TCEP day, each group has totally 25 points at 5 time points for the 5 TC tracks. The average tracks of each group (green line in Fig. 10) are determined by the average in 5 time points. The 'composite' is performed by dynamic composite analysis that synthesizes horizontal wind field at 850 hPa by tracing 25 centers of progressive TCs on the TCEP day. For each group, we calculated the average of a total of 25 points to get the average TC center. Considering the relationship between the average TC center and the map, we can draw Fig. 10.

Comparing Fig. 10a, b, while the direction of the STG average track was between northwest and north, the WTG track was northwest. The moving direction of the TCs may have had an effect on the TCEP intensity in Central R-HFLT. The STG produced more concentrated TCMDTR locations on the landfall day than WTG. On the TCEP day, the average low-level circulation of STG at 850 hPa was stronger than that of WTG, with the R-HFLT circulation center of STG locates on landfall, while R-HFLT circulation center of WTG was already onshore. Track of STG is consistent with the expectation that the wind-terrain interaction may play a great role on the TCEP day of STG because the TC centers are over land, which is in coincidence with the result that the largest terrain effect should be in the overland phase when TC landfall (Chang et al. 2013).

Apart from the terrain and track factors, the individual characteristics of each TC had an important function in the formation of TCEP. Differences between the two TC

Table 2 Comparisons of the two central-type TC groups [strong central-type TCs group (STG) and weak central-type TCs group (WTG)] on the TCEP day over Southeast China

Names of STG	Extreme values (mm)	Station of occurrence	Names of WTG	Extreme values (mm)	Station of occurrence
05Haitang	472.5	Zherong	94 Gladys	155.8	Suburb of Fuzhou
09Morakot	415.2	Zherong	97 Amber	166.9	Zherong
71Bess	322.1	Zherong	12 Saola	189.9	Pingtan
62Opal	281.6	Luoyuan	80 Norris	160.4	Fuqing
08Fung-wong	266.9	Zherong	69 Betty	158.4	Lianjiang

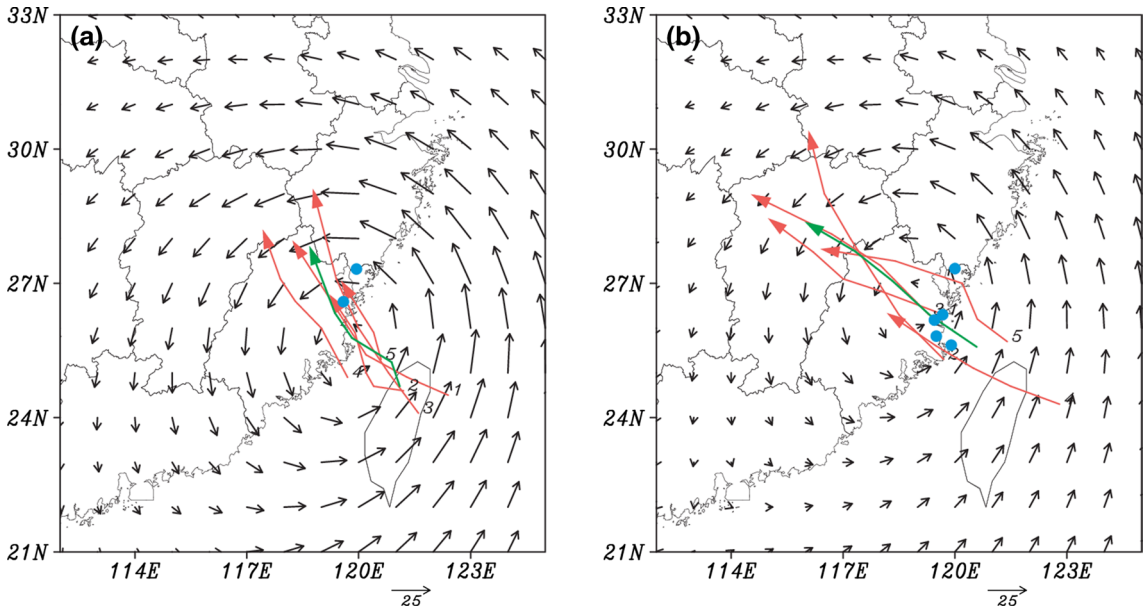

Fig. 10 Composite horizontal wind field at 850 hPa (vectors, units: m/s), TC track (red lines indicate group TC members, and the green line indicates the average track of each group), and TCMDTR distribution (blue dots) on the TCEP day for (**a**) strong central-type TC group (STG); and (**b**) weak central-type TC group (WTG)

groups, including TCEP intensity, strength, moving speed, and track direction, are quantified in Fig. 11. The average TCEP intensity reached 351.7 mm for STG, and 160.0 mm for WTG. Many of the largest rainfall events associated with tropical cyclones have occurred when this storm translation speed was small (Lee et al. 2011). The average translation speed of WTG was nearly 1.5 times that of STG. In addition, examining the relationship between the translation speed and TCEP intensity from all TCs affecting Central R-HFLT, we find that the slower the velocity and the greater the TCEP, with correlation coefficient of about − 0.4 at the 0.01 significance level. The intensity of the two TC groups varied greatly, while the average intensity of STG reached 48 m/s compared with 33.6 m/s for WTG. The statistical analysis between TC intensity and TCEP intensity indicates a slightly positive correlation, which is up to a significant level of 0.05. For the track direction of the track, we made a connection from the start to the end point of the average tracks (green line) in Fig. 10. Treating due west as 0°, the track direction was defined by rotating the connection vector in the anticlockwise direction. The average track direction of STG was approximately 304.3°, while the WTG average track direction was 324.5°. Compared with the average track of the WTG track, that of the STG track has a larger northern component and a position closer to the terrain. The average horizontal wind at 850 hPa for the STG track is easterly or southeasterly (Fig. 10a), making the station where the TCMDTR occurs located on the windward slope of the terrain and on the right side of landfalling track. However, the average horizontal wind at 850 hPa for the WTG track is southerly or southwesterly (Fig. 10b), which indicates that the configuration of the track and the terrain for WTG track is not as good as that of the WTG track. Thus, the comparison of the two groups of the central type indicates that TCs with a slower translation speed, stronger intensity, and a more northerly track contributed to heavier TCEP. Especially, the STG track matched well with the terrain, which played an important role in the TCEP distribution. As a whole, under a more northerly moving direction and slow movement, together with the unique terrain, the TCs with a stronger vortex circulation generated heavier TCEP during landfall in Central R-HFLT.

In addition to the TC features, we also examined the role of the background environment, which is thought to be an important external factor accounting for TCEP. The average environmental circulation during the TCEP day was obtained for the two TC groups by dynamic composite analysis. A fairly good contrast was found between the environments of the two TC groups at different levels.

On lower environmental field, Fig. 12 shows the average moisture flux and composite horizontal wind associated with the two TC groups at 850 hPa. For both STG and WTG, there was a southwest airflow with moisture supply from the low-latitude ocean (10°N nearby) in connection with the typhoon circulation during the landfall, where WTG's moisture channel is even stronger somewhere. However, in the vicinity of the TC center, STG is related to a stronger moisture flux, which provides adequate moisture and leads to

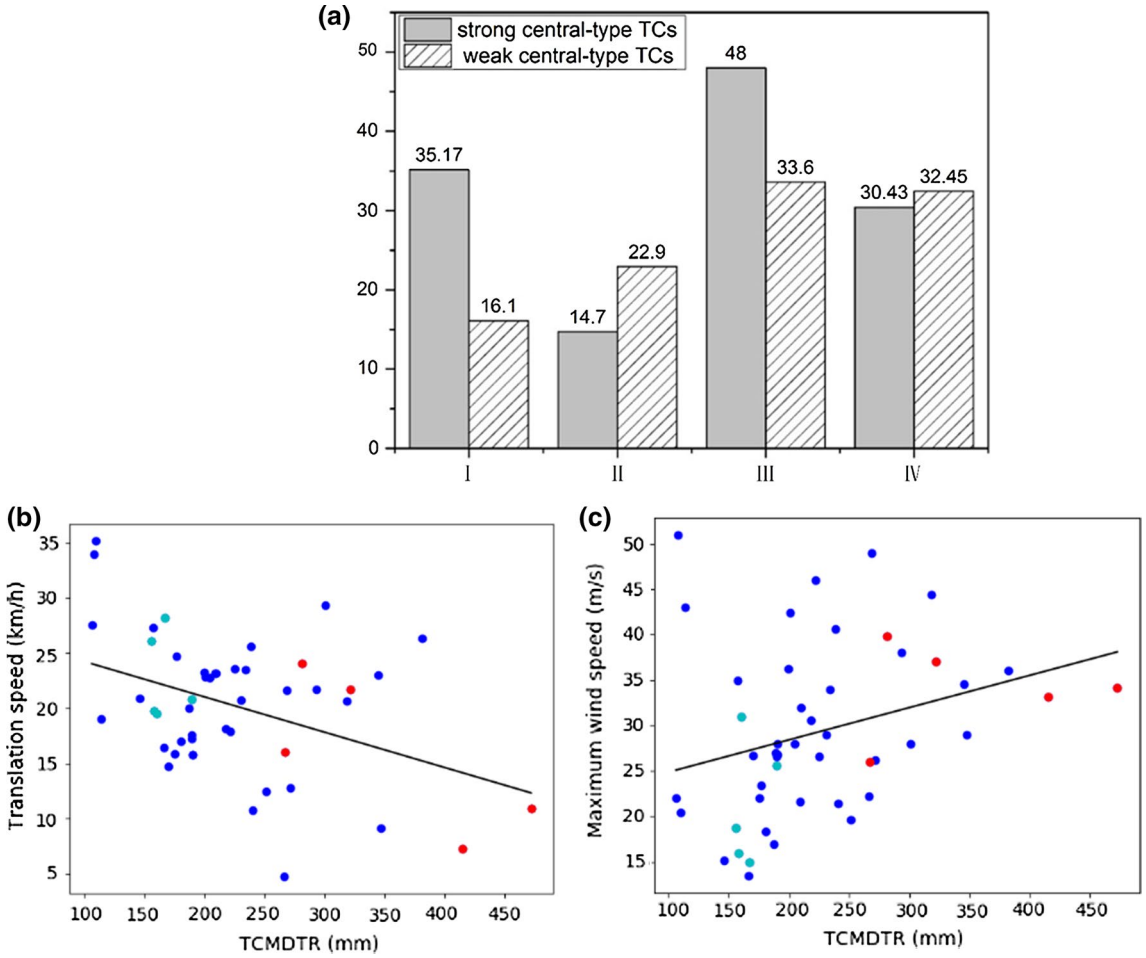

Fig. 11 Characteristic statistics of influence TCs for Central R-HFLT on the TCEP days. **a** Characteristic statistics for the strong and weak central-type TC groups. I, II, III, and IV represent TCEP intensity (units: 10 mm), translation speed (units: km/h), maximum wind speed (units: m/s), and track direction (units: 10°), respectively. **b** Distribution of TC translation speed (units: km/h) and TCEP intensity (units: mm) for all TCs bringing TCEP ≥ 100 mm in Central R-HFLT, with red (cyan) dots indicating STG (WTG). **c** As (**b**), but for TC intensity (m/s)

Central R-HFLT wetter (Fig. 12a). Having a potential moisture supply, the STG could maintain a wide range of heavy rainfall, while the moisture in Central R-HFLT accompanying the landfalling WTG was relatively weaker (Fig. 12b). In addition, the moisture convergence inside the STG was longer lasting, which could promote TC rainfall. According to Chen et al. (2010), a strong TC can maintain and produce strong precipitation through its internal process during landfall, while a weaker TC requires good environmental conditions to produce strong precipitation. Comparing the two TC groups, STG had better moisture conditions than WTG, which showed that sufficient moisture was necessary for TCEP.

Composite horizontal wind and geopotential height fields at 500 hPa are depicted in Fig. 13. In the STG environment, a westerly trough occurred to the east of Lake Baikal in the high latitudes, exhibiting strong radial circulation. Located at the bottom of the East Asian trough controlling the whole of East Asia, STG tended to travel north. A westerly trough may have channeled some cold air southward into the northern part of the TC circulation, increasing heat, triggering the release of unstable energy, and increasing TCEP intensity. However, the WTG background had a relatively flat airflow and the subtropical high was fused with mainland high pressure, which was conducive to the more westerly track (Fig. 10b) and a large translation speed for WTG (Fig. 11). Therefore, the STG at 500 hPa was more conducive to precipitation extremes than WTG.

In the wind fields at 200 hPa (not shown), relative to the weak divergence with WTG at a high level, STG corresponded with an obvious divergent situation, which was favorable to the maintenance of a TC. Coupled with the water vapor flux convergence at 850 hPa, a good configuration was formed, which was favorable to the secondary

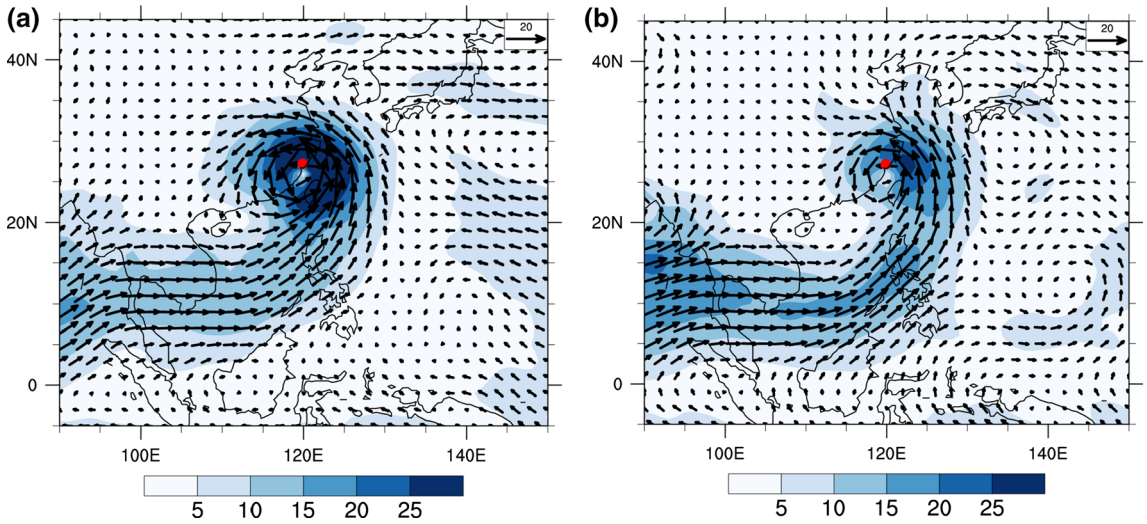

Fig. 12 Distributions of composite horizontal wind (vectors, units: m/s) and vapor flux [shaded, units: g/(cm hPa s)] fields at 850 hPa averaged over the TCEP day for **a** strong central-type TCs, and **b** weak central-type TCs

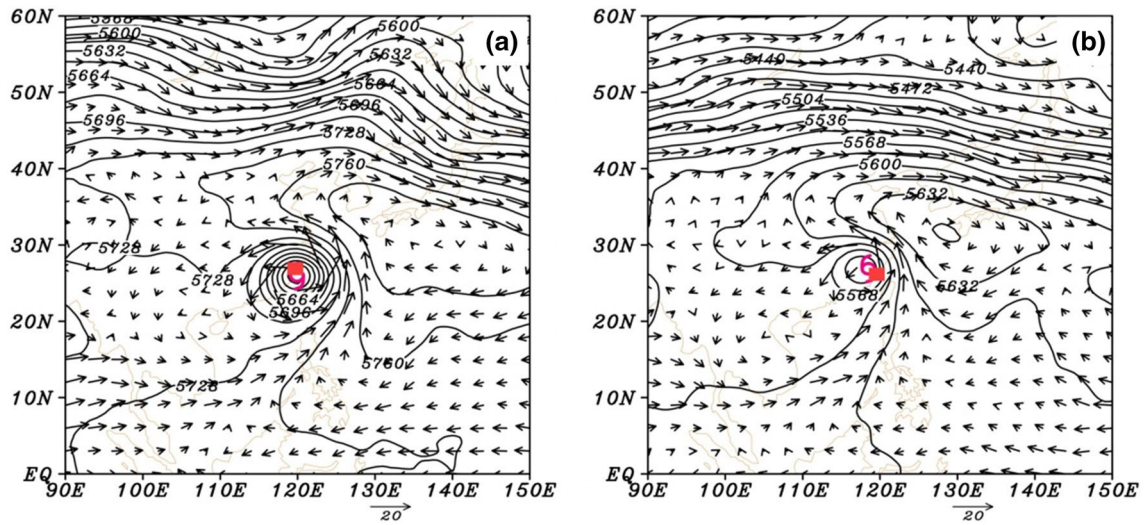

Fig. 13 Distributions of composite horizontal wind (vectors, units: m/s) and geopotential height (contours, units: gpm) fields at 500 hPa averaged over the TCEP day for **a** strong central-type TCs, and **b** weak central-type TCs

circulation in TCs and the development of convective systems, resulting in heavier TCEP. These statistics are consistent with previous work and further investigations are under way.

The preliminary results suggest that the interaction of the TC circulation with special terrain was the main factor, while the characteristics of TCs and the interaction between the TCs and other weather systems also promoted the formation of heavy TCEP.

5 Summary and discussion

The extreme precipitation associated with TC activity often causes disasters in Southeast China. Numerical simulations of TCs in a warmer climate suggest that TC-related rainfall rates are likely to increase (Knutson et al. 2010). Although case studies show widespread increases in heavy precipitation events, the regional TCEP change

in Southeast China has not been well understood in observational studies. Using daily precipitation observations at 157 meteorological stations during 1958–2016, we investigated the primary regional characteristics of TCEP in Southeast China, with a special focus on the climatic variation of TC case maximum daily precipitation (TCMDTR) and the spatial distribution of station maximum daily precipitation (SDTR) identifying some preliminary causes.

Over recent decades, the intensity and frequency of high-intensity TCEP (≥ 100, ≥ 200, ≥ 300 mm) have increased. Although influential TCs with TCMDTR above 50 mm over Southeast China have decreased over the past 59 years, the frequency of TCs with TCMDTR above 100 mm suggests a significant increasing trend with time. The greater the TCEP intensity, such as 200 or 300 mm and above, the more obvious the trend. Monthly change was characterized by a single peak during July–September, with frequency peaks in August for TCMDTR at all intensity levels, except for the TCMDTR ≥ 300 mm frequency, which peaked in September. This indicates that Southeast China is more likely to be affected by severe TCEP in September.

The TCEP showed an uneven spatial distribution, with a ladder trend from the coast to inland. The heavy TCEP and high frequency of TCEP ≥ 100 mm were concentrated near the coast, forming three extreme R-HFLTs: the southern Fujian region (Southern R-HFLT), the northern Fujian region (Central R-HFLT), and the region around southern Zhejiang (Northern R-HFLT). With the increase in strength, the Central R-HFLT tended to experience high frequencies.

Terrain was the main cause of TCEP on the southeast coast. The three extreme R-HFLTs matched the terrain, with the Central R-HFLT coinciding with the coastal area from South Yandang Hill in Southern Zhejiang to the northeast of Jiufeng Mountains in Northeast Fujian; the Northern R-HFLT corresponding to the North Yandang Hill in the central areas of Zhejiang; and the Southern R-HFLT was located in the central-to-southern coast of the Daiyun Mountains in Fujian. In particular, the "pocket" terrain in the Central R-HFLT made the frequency and magnitude of TCEP at Zhenrong station much greater than those at the other stations, which shows the significant role of the topography effect in the climatological TCEP of Southeast China.

Analyzing the causes of TCEP in Central R-HFLT, we found that TCs with greater intensity, slower translation speed, and more northerly moving direction generated stronger TCEP. Great TCEP occurred when easterly and southeasterly winds interact with terrain over the eastern coast of Central R-HFLT for the central-type TCEP. The more northerly track together with the effect of topography caused an increase in the intensity and frequency of the TCEP. These large TCEP intensities are also in coincidence with the interactions between the easterly (or southeasterly) winds and the terrain over Central R-HFLT coast, which agrees with Chang et al. (2013). As the STG (WTG) discussed here is somewhat similar to the typhoon in the overland (exit) phase in Chang et al. (2013), the interaction between the overland-phase TCs (STG) and the terrain is more obvious, resulting in heavier TCEP.

In addition, the corresponding environment of the Central R-HFLT was more conducive to TCEP, with abundant low-level moisture convergence, divergence at high level, and favorable mid-latitude conditions. In summary, the terrain, the TC features, and the external environment were all inseparable as causes for TCEP in Southeast China during 1958–2016.

This study revealed some of the preliminary characteristics of TCEP in Southeast China; however, further study is needed on the causes of the climatological variation and spatial characteristics, and the causes of the terrain require more numerical simulation for quantitative results and verification.

Acknowledgements This work was supported by the Chinese Ministry of Science and Technology Project (Grant 2015CB452806) and the National Natural Science Foundation of China (Grants 41375056, 41675042). This work is also supported by China Scholarship Council.

References

Burpee RW, Black ML (1989) Temporal and spatial variations of rainfall near the centers of two tropical cyclones. Mon Weather Rev 117:2204–2218

Chan JCL, Liu KS, Ching SE et al (2004) Asymmetric distribution of convection associated with tropical cyclones making landfall along the South China coast. Mon Weather Rev 132:2410–2420

Chang CP, Lei Y, Sui CH, Lin X, Ren F (2012) Tropical cyclone and extreme rainfall trends in East Asian summer monsoon since Mid-20th Century. Geophys Res Lett 39:L18702. https://doi.org/10.1029/2012GL052945

Chang CP, Yang YT, Kuo HC (2013) Large increasing trend of tropical cyclone rainfall in Taiwan and the roles of terrain. J Clim 26:4138–4147. https://doi.org/10.1175/JCLI-D-12-00463.1

Chen L (2007) Research and forecast on tropical cyclone landfall heavy rainfall. In: The 14th national tropical cyclone scientific symposium abstract book. pp 3–7 **(in Chinese)**

Chen L, Ding Y (1979) Introduction to typhoon in north western pacific, China Science Press, Beijing, p 491

Chen L, Li Y, Cheng Z (2010) An overview of research and forecasting on rainfall associated with landfalling tropical cyclones. Adv Atmos Sci 27:967–976

Chen L, Luo Z, Li Y (2004) Research advances on tropical cyclone landfall process. Acta Meteor Sin 62:541–549

Cheng Z, Chen L, Liu Y et al (2007) The spatial and temporal characteristics of tropical cyclone-induced rainfall in China during 1960–2003. J Appl Meteorol Sci 18:427–434 **(in Chinese)**

Cheung KKW, Huang LR, Lee CS (2008) Characteristics of rainfall during tropical cyclone periods in Taiwan. Nat Hazards Earth Syst Sci 8:1463–1474

Gao SZ, Meng ZY (2009) Observational analysis of heavy rainfall mechanisms associated with Severe Tropical Storm Bilis (2006) after its landfall. Mon Weather Rev 137:1881–1897

Ge XY, Li T, Zhang SJ, Peng M (2010) What causes the extremely heavy rainfall in Taiwan during Typhoon Morakot (2009)? Atmos Sci Lett 11:46–50

Gray WM (1981) Recent advances in tropical cyclone research from rawinsonde composite analysis. WMO Program on Research in Tropical Meteorology, Fort Collins, p 407

Jiang H, Zipser EJ (2010) Contribution of tropical cyclones to the global precipitation from eight seasons of TRMM data: regional, seasonal, and interannual variations. J Clim 23:1526–1543

Knight DB, Davis RE (2007) Climatology of tropical cyclone rainfall in the Southeastern United States. Phys Geogr 28:126–147

Knight DB, Davis RE (2009) Contribution of tropical cyclones to extreme rainfall events in the Southeastern United States. J Geophys Res 114:D23102. https://doi.org/10.1029/2009JD012511

Knutson TR, McBride JL, Chan J et al (2010) Tropical cyclones and climate change. Nat Geosci 3:157–163

Kubota H, Wang B (2009) How much do tropical cyclones affect seasonal and interannual rainfall variability over the western north pacific? J Clim 22:5495–5510

Larson J, Zhou Y, Higgins RW (2005) Characteristics of landfalling tropical cyclones in the United States and Mexico: climatology and interannual variability. J Clim 18:1247–1262

Lee CS, Wu CC, Wang TCC, Elsberry RL (2011) Advances in understanding the "perfect monsoon-influenced typhoon": summary from international conference on Typhoon Morakot (2009). AsiaPac J Atmos Sci 47:213–222. https://doi.org/10.1007/s13143-011-0010-2

Li Y, Chen L, Wang J (2004) The diagnostic analysis on the characteristics of large scale circulation corresponding to the sustaining and decaying of tropical cyclone after it's landfall. Acta Meteor Sin 62:167–179 **(in Chinese)**

Li RCY, Zhou W, Lee TC (2015) Climatological characteristics and observed trends of tropical cyclone-induced rainfall and their influences on long-term rainfall variations in Hong Kong. Mon Weather Rev 143:2192–2206

Lin YL, Ensley DB, Chiao S (2002) Orographic influences on rainfall and track deflection associated with the passage of a tropical cyclone. Mon Weather Rev 130:2929–2950

Lin, YY, Liu YQ, Zhang LQ (2001) An analysis on the impact of severe tropical storm "Maria" on the torrential heavy rain in Shaoguan. Guangdong Meteor 3:5–7

Liu KS, Chan JCL, Cheng WC et al (2007) Distribution of convection associated with tropical cyclones making landfall along the South China coast. Meteorol Atmos Phys 97:57–68

Liu T, Wu L, Zhang J, Ren F (2013) Analysis of tropical cyclone precipitation changes in China in July–September during 1965–2010. Acta Meteor Sin 71:63–75 **(in Chinese)**

Marks FD (1985) Evolution of the structure of precipitation in Hurricane Allen (1980). Mon Weather Rev 113:909–930

Meng WG, Wang Y (2016) A diagnostic study on heavy rainfall induced by typhoon utor (2013) in south China: 1. rainfall asymmetry at landfall. J Geophys Res Atmos 121. https://doi.org/10.1002/2015JD024646

Ren F, Gleason B, Easterling D (2001) A numerical technique for partitioning cyclone tropical precipitation. J Trop Meteorol 17:308–313

Ren F, Wu G, Dong W, Wang X, Wang Y, Ai W, Li W (2006) Changes in tropical cyclone precipitation over China. Geophys Res Lett 33:L20702. https://doi.org/10.1029/2006GL027951

Ren F, Qiu W, Jiang X et al (2017) An objective index for identifying tropical cyclone track similarity. Weather and Forecasting (editing)

Rodgers EB, Adler RF, Pierce HF (2000) Contribution of tropical cyclones to the north pacific climatological rainfall as observed from satellites. J Appl Meteorol 39:1658–1678

Rodgers EB, Adler RF, Pierce HF (2001) Contribution of tropical cyclones to the North Atlantic climatological rainfall as observed from satellites. J Appl Meteorol 40:1785–1800

Shah BV (1983) Is the environment becoming more hazardous?—A global survey 1947 to 1980. Disasters 7:202–209

Su Z, Ren F, Wei J, Lin X, Shi S, Zhou X (2016) Changes in monsoon and tropical cyclone extreme precipitation in southeast China from 1960 to 2012. Trop Cyclone Res Rev 4:12–17. https://doi.org/10.6057/2015TCRR01.02

Webster PJ, Holland GJ, Curry JA et al (2005) Changes in tropical cyclone number, duration, and intensity in a warming environment. Science 309:1844–1846

Wu L, Zhao HK (2012) Dynamically derived tropical cyclone intensity changes over the western North Pacific. J Clim 25:89–98

Wu CC, Yen TH, Kuo YH, Wang W (2002) Rainfall simulation associated with typhoon Herb (1996) near Taiwan. Part I: the topographic effect. Weather Forecast 17:1001–1015

Wu L, Wang B, Geng S (2005) Growing typhoon influence on east Asia. Geophys Res Lett 32:L18703. https://doi.org/10.1029/2005GL022937

Wu Y, Wu S, Zhai P (2007) The impact of tropical cyclones on Hainan Island's extreme and total precipitation. Int J Climatol 27:1059–1064

Wu L, Liang J, Wu CC (2011) Monsoonal influence on Typhoon Morakot (2009). Part I: observational analysis. J Atmos Sci 68:2208–2221

Wu CC, Yen TH, Huang YH, Yu CK, Chen SG (2016) Statistical characteristic of heavy rainfall associated with typhoon near Taiwan based on high-density automatic rain gauge data. Bull Am Meteorol Soc 97:1363–1375. https://doi.org/10.1175/BAMS-D-15-00076.1

Xie B, Zhang F (2012) Impacts of typhoon track and island topography on the heavy rainfalls in Taiwan associated with Morakot (2009). Mon Weather Rev 140:3379–3394

Ying M, Chen B, Wu G (2011) Climate trends in tropical cyclone-induced wind and precipitation over mainland China. Geophys Res Lett 38:L01702. https://doi.org/10.1029/2010gl045729

Yu CK, Cheng LW (2013) Distribution and mechanisms of orographic precipitation associated with Typhoon Morakot (2009). J Atmos Sci 70:2894–2915

Yue C, Shou S, Zeng G et al (2008) Preliminary study on asymmetric cause of formation of precipitation associated with typhoon Haitang. Plateau Meteorol 27:1333–1342 **(in Chinese)**

Zhang Q, Liu Q, Wu L (2009) Tropical cyclone damages in China 1983–2006. Bull Am Meteorol Soc 90:489–495. https://doi.org/10.1175/2008BAMS2631.1

Zhang J, Wu L, Ren F et al (2013) Changes in tropical cyclone rainfall in China. J Meteorol Soc Jpn 91:585–595. https://doi.org/10.2151/jmsj.2013-502

Zhu P, Zheng Y, Zheng P (2010) Asymmetric distribution of convection associated with tropical cyclone making landfall along the east China coast. J Trop Meteorol 26:651–658 **(in Chinese)**